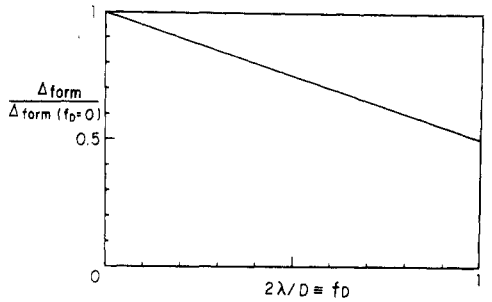

Figure 9. Form birefringence of a pseudo-two-phase system as a function of interfacial volume fraction $f_D = 2\lambda/D$. The form birefringence relative to the ideal two-phase system Δ_{form} (f_D = 0) is plotted for the case where $\phi_A(z)$ is given by eq III-13. Δ_{form} was calculated from eq III-20b.

may become quite large for systems in which the two block chains have large segmental anisotropies with same sign.

Figure 9 shows the effect of the interface on form birefringence for the case where the polystyrene and polyisoprene lamellae are optically isotropic and the density profile across the interface is given by eq III-13. In this case Δ_{form} is equal to Δn_t in eq III-20 with $f_A = f_B = (1 - f_D)/2$, $n_{Ax} = n_{Az} = \bar{n}_A$, and $n_{Bx} = n_{Bz} = \bar{n}_B$, where f_D is the volume fraction of the interface ($f_D = 2\lambda/D$). It is clearly seen that the absolute value of the form birefringence decreases with increasing volume fraction of the interface. When $2\lambda/D = 1$, the form birefringence becomes as low as half of the value with zero interfacial thickness, i.e., when $2\lambda/D = 0$.

Acknowledgment. This work was supported by the NSF (National Science Foundation) and the JSPS (Japan Society of Promotion of Science) under the US–Japan Joint Research Program during the period 1981–1982.

Registry No. (Isoprene)·(styrene) (copolymer), 25038-32-8.

References and Notes

(1) Meier, D. J. *J. Phys. Chem.* **1967**, *71*, 1861.
(2) Meier, D. J. *Appl. Polym. Symp.* **1974**, *24*, 67.
(3) Meier, D. J. *Prepr. Polym. Colloq., Soc. Polym. Sci. Jpn., Kyoto* **1977**, 83.
(4) Kuhn, W.; Grün, F. *Kolloid Z.* **1942**, *101*, 248.
(5) Treloar, L. R. G. *Trans. Faraday Soc.* **1947**, *43*, 277.
(6) Wiener, O. *Abh. Math.-Phys. Kl. Saechs. Ges. Wiss.* **1912**, *32*, 507.
(7) Cvikl, B.; Moroi, D.; Franklin, W. *Mol. Cryst. Liq. Cryst.* **1971**, *12*, 267.
(8) Hashimoto, T.; Todo, A.; Hashimoto, K.; Kawai, H. *Rep. Prog. Polym. Phys. Jpn.* **1977**, *20*, 461.
(9) Brandrup, J., Immergut, E. H., Eds. "Polymer Handbook"; Wiley: New York, 1975; Chapter 4.
(10) Hashimoto, T.; Shibayama, M.; Kawai, H. *Macromolecules* **1980**, *13*, 1237.
(11) Folkes, M. J.; Keller, A. *Polymer* **1971**, *12*, 222.
(12) Cahn, J. W.; Hilliard, J. E. *J. Chem. Phys.* **1958**, *28*, 258.
(13) Helfand, E.; Tagami, Y. *J. Polym. Sci., Part B* **1971**, *9*, 741.
(14) Helfand, E. *Acc. Chem. Res.* **1975**, *8*, 295.
(15) Hopper, R. W.; Uhlmann, D. R. *J. Colloid Interface Sci.* **1974**, *47*, 77.
(16) Roe, R. J. *J. Chem. Phys.* **1975**, *62*, 490.

Uniformity of Microdomain Size of Block Polymers As Compared with Uniformity of Their Molecular Weights

Takeji Hashimoto,* Hideaki Tanaka, and Hirokazu Hasegawa

Department of Polymer Chemistry, Faculty of Engineering, Kyoto University, Kyoto 606, Japan. *Received December 11, 1984*

ABSTRACT: The uniformity of the microdomain sizes of polystyrene–polyisoprene block polymers is found to be much higher than the uniformity of molecular weights of the block polymers comprising the microdomains; the heterogeneity index for the distribution of microdomain size ($\bar{D}_w/\bar{D}_n$) is typically 1.001, while that for the molecular weight distribution of the block polymers studied ($\bar{M}_w/\bar{M}_n$) is typically 1.1 ($\bar{D}_w$ and $\bar{D}_n$ are the weight- and number-average domain identity periods and $\bar{M}_w$ and $\bar{M}_n$ are the corresponding average molecular weights). This implies that the molecules are packed in the domain space so as to compensate their molecular weight distributions.

Introduction

In this paper we are concerned with uniformity of the microdomain sizes of typical block polymers such as polystyrene–polyisoprene block polymers as compared with that of the molecular weights of the polymers comprising the microdomains. We wish to emphasize that the uniformity of the former is higher than that of the latter (e.g., $\bar{D}_w/\bar{D}_n \simeq 1.001$ and $\bar{M}_w/\bar{M}_n \simeq 1.1$; see eq 10 and 11) and that the molecules are packed in the domain space so as to compensate for the molecular weight and compositional distributions.

It is well-known that block polymers exhibit microdomain structures in the strong segregation limit. The size of these microdomains has to be closely related to the size of individual molecules,[1-9] the physics of which originates from the incompressibility of polymeric liquids and solids.[10,11] Incompressibility demands that the segments uniformly fill all space of the microdomains and their densities in the respective microphases should be equal to those in the corresponding homopolymers. Thus the molecules in the domain space have to adjust their dimensions and conformations according to the size of the microdomains as schematically shown in Figure 1. For example, if the domain space composed of A molecules expands from D_{A1} to D_{A2}, the A block molecules also have to expand their dimensions (with the root-mean-square end-to-end distance from $\langle Z_{A1}^2\rangle^{1/2}$ to $\langle Z_{A2}^2\rangle^{1/2}$) in the direction perpendicular to the interface in order to satisfy the demands of uniform space filling with the segments. The expansion of the molecules has to be accompanied by a decrease of the average intermolecular distance from a_1 to a_2 in order to satisfy the demands invoked by incompressibility. The equilibrium domain size is the one which minimizes the free energy of the system.

It has been found both theoretically and experimentally that the microdomain size (R_A) and the identity period (D)

0024-9297/85/2218-1864$01.50/0

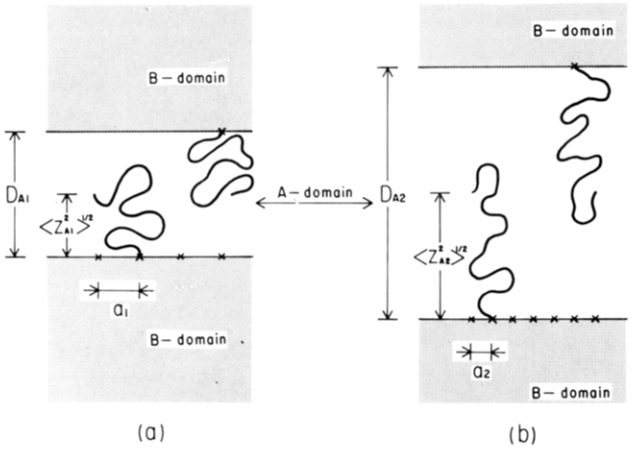

Figure 1. Relationship between the size of the microdomain (D_{A1} and D_{A2}) and the size of the block polymer chain ($\langle Z_{A1}^2 \rangle^{1/2}$, $\langle Z_{A2}^2 \rangle^{1/2}$) comprising the microdomain. a_1 and a_2 are the average nearest-neighbor distances of the chemical junctions of A–B diblock polymers along the interface.

of the periodically arranged microdomains have molecular weight dependences as given by[3-5]

$$R_A \sim M_A^{2/3} \tag{1a}$$

$$D \sim M^{2/3} \tag{1b}$$

for A–B and A–B–A type block polymers composed of polystyrene and polyisoprene or polybutadiene in the equilibrium regime.[12,13] Equation 1 was found to be applicable to all morphologies, i.e., spherical,[4] cylindrical,[5] and lamellar microdomains.[3] Here M_A and M are the number-average molecular weights of the A block chains and of the total block polymers, respectively. If two block polymers with different molecular weights but with the same constituent polymers A and B are mixed and if they are molecularly mixed in a single type of microdomain,[6] R_A and D are found experimentally to be given by replacing M in eq 1 by M_n, the number-average molecular weight of the two block polymers.[7]

$$R_A \sim \bar{M}_{n,A}^{2/3} \tag{2a}$$

$$D \sim \bar{M}_n^{2/3} \tag{2b}$$

In this paper we attempt to analyze the uniformity of the domain size as compared with the uniformity of the molecular weight distributions. Although rigorously the parameter evaluated in our experiment is not the domain size D_A or D_B of A–B block polymer, but the domain spacing D, these parameters are interrelated with each other and are not independent. For a given molecular weight and composition, the connectivity of A and B block chains and the incompressibility of polymeric liquids lead to the relationships

$$D = 2(N/S)(v_A + v_B) = 2(N/S)(M_A/\rho_A N_A + M_B/\rho_B N_A)$$

$$D_A = 2(N/S)v_A = 2(N/S)M_A/\rho_A N_A$$

$$D_B = 2(N/S)v_B = 2(N/S)M_B/\rho_B N_A$$

where N is the total number of polymer chains, S the total interfacial area, N_A Avogadro's number, and v_K, M_K, and ρ_K are the molecular volume, molecular weight, and mass density of K block chains, respectively. Thus the same level of fluctuations are expected for D, D_A, and D_B if the distributions of M_A and M_B are on the same level as that of total molecular weight M. This is a reasonable assumption for anionically polymerized polystyrene–polyisoprene or polystyrene–polybutadiene block polymers

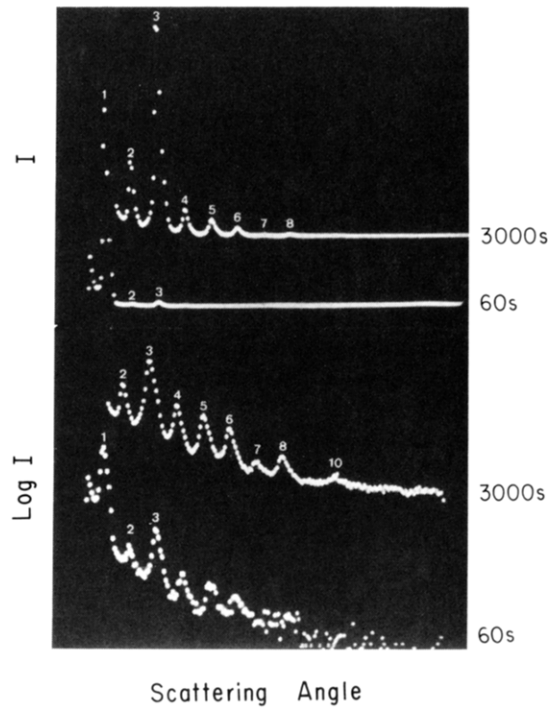

Figure 2. Oscilloscope displays of typical SAXS profiles from the solvent-cast films of SIL-1. The SAXS intensity data are displayed on a linear scale for the upper two curves, while they are displayed on a logarithmic scale for the lower two curves. The profiles were measured with 60- or 3000-s exposure to X-rays.

since side reactions hardly occur during their polymerizations. Besides this argument, it is generally expected that the domain spacing D fluctuates as a consequence of fluctuations of the respective domain sizes D_A and D_B and that the fluctuations of D_A and D_B are mutually related because of the connectivity of A and B block chains. Hence the fluctuation of D reflects the fluctuation of domain size D_A or D_B.

Experimental Section

The block polymers considered here are those prepared by sequential living anionic polymerization. Such A–B and A–B–A type block polymers of polystyrene (PS) and polyisoprene (PI) or polybutadiene (PB) are uncontaminated by homopolymer impurities and are amorphous. In addition, we present here results on a particular PS–PI diblock polymer designated as SIL-1 and having a total number-average molecular weight ($\bar{M}_n$) of 9.4×10^4 and weight fraction of PS (W_{PS}) equal to 0.5.

The block polymers were dissolved in toluene, a good solvent for both block components, and films were prepared by casting 10% solutions onto a glass plate in the manner described in detail elsewhere.[3] The small-angle X-ray scattering and electron microscopic observations were also made in the same manner described elsewhere.[3]

Results and Discussion

The electron microscopic observations indicated the existence of alternating lamellar microdomains of PS and PI for the test film prepared from SIL-1. The film exhibited a single lamellar morphology with a single identity period $\bar{D}$ and single lamellar thicknesses ($\bar{D}_{PS}$ and $\bar{D}_{PI}$ for PS and PI lamellae, respectively) over the whole sample.

Small-angle X-ray scattering (SAXS) investigations with pinhole collimation indicated that the lamellae in each test film were highly oriented with their interfaces parallel to the film surfaces to a degree, as described elsewhere.[3] Figure 2 shows oscilloscope displays of the SAXS profiles measured with the SAXS camera[14,15] with a position-sensitive proportional counter in the direction perpendicular to the film surfaces. Although the profiles were uncor-

rected for absorption, air scattering, and slit-width smearing, they were sufficient to show the existence of very regular and long-range spatial order of the lamellar microdomains. The upper two curves (measured with 3000- and 60-s exposure to the X-rays, respectively) are the profiles for which the number of photons for the scattered X-rays (proportional to SAXS intensity) are plotted on a linear scale as a function of the channel number of the multichannel analyzer (corresponding to the scattering angles). In the lower two curves (measured again with 3000- and 60-s exposure to the X-rays), the intensity was plotted on a logarithmic scale. The first-order scattering maximum is shown in the curves measured with 60-s exposure to X-rays but not in those measured with 3000 s because of the overscale of the maximum intensity. The number marked at each maximum corresponds to the order of higher order scattering maxima from a single lamellar identity period $\bar{D}$. At least up to 10th-order maximum can be resolved for this particular block polymer sample.

The SAXS profile from a test specimen having a lamellar morphology generally shows a number of higher order scattering maxima arising from a single identity period $\bar{D}$, satisfying

$$2\bar{D} \sin \theta = n\lambda \qquad (n = \text{integer}) \tag{3a}$$

$$s\bar{D} = n \qquad (s = (2 \sin \theta)/\lambda) \tag{3b}$$

where λ is the wavelength of the X-rays and 2θ is the scattering angle. The spacing $\bar{D}$ for SIL-1 was estimated to be 460 Å. It should be noted that most block polymer films having a lamellar morphology exhibit a number of higher order diffractions.[3,8] The number of higher order maxima seem to decrease with decreasing molecular weight of the block polymers, i.e., with decreasing D. However, this is primarily because a given higher order maximum for the block polymers with lower molecular weights tends to appear at higher scattering angle and therefore tends to be affected by the background scattering arising from the thermal diffuse scattering. In other words, the scattering maxima appearing at large scattering angles tend to be buried in the background scattering level and therefore cannot be resolved.

Uniformity of Domain Size

According to Hosemann's paracrystal theory of diffraction,[16] the nth-order diffraction maximum is distinguishable if

$$gn \lesssim 0.35 \tag{4}$$

where

$$g \equiv \sigma_D/D \tag{5a}$$

with

$$\sigma_D^2 = \langle (D - \bar{D})^2 \rangle \tag{5b}$$

and σ_D^2 is the mean-square deviation of the domain identity period D from the mean value $\bar{D}$. Knowing the g value, one can estimate the heterogeneity for the distribution of D, $[\mathrm{HI}]_D$, which is defined as a ratio of weight-average D ($\bar{D}_w$) and number-average D ($\bar{D}_n$)

$$[\mathrm{HI}]_D \equiv \bar{D}_w/\bar{D}_n \tag{6}$$

where

$$\bar{D}_w \equiv \int_0^\infty D^2 W(D)\, dD / \int_0^\infty D W(D)\, dD = \overline{D^2}/\bar{D} \tag{7}$$

$$\bar{D}_n \equiv \int_0^\infty D W(D)\, dD / \int_0^\infty W(D)\, dD = \bar{D} \tag{8}$$

where $\bar{D}$ and $\overline{D^2}$ are the first and second moments of the distribution function $W(D)$. From eq 6–8, it is obvious that

$$[\mathrm{HI}]_D = \overline{D^2}/\bar{D}^2 = (\sigma_D/\bar{D})^2 + 1 = g^2 + 1 \tag{9}$$

For the specimens which exhibit up to 10th, 5th, 2nd-, and 1st-order scattering maximum, g is approximately 0.035, 0.07, 0.175, and 0.35, respectively (see eq 4). Consequently these specimens may have $[\mathrm{HI}]_D$ as follows:

$$[\mathrm{HI}]_D = 1.001 \quad \text{for } g = 0.035 \quad (n = 10) \tag{10a}$$

$$[\mathrm{HI}]_D = 1.005 \quad \text{for } g = 0.07 \quad (n = 5) \tag{10b}$$

$$[\mathrm{HI}]_D = 1.031 \quad \text{for } g = 0.175 \quad (n = 2) \tag{10c}$$

$$[\mathrm{HI}]_D = 1.123 \quad \text{for } g = 0.35 \quad (n = 1) \tag{10d}$$

The block polymer SIL-1, whose SAXS profiles are shown in Figure 2, exhibits at least up to a 10th-order scattering maximum and hence has $[\mathrm{HI}]_D \simeq 1.001$. The other block polymers, having molecular weights of the order of 10^5 and having the lamellar morphology, also usually exhibit up to about 10th-order maximum[17] and hence have about the same uniformity in D. On the other hand, the heterogeneity $[\mathrm{HI}]_M$ for the molecular weight distribution of these polymers is usually much larger

$$[\mathrm{HI}]_M = \bar{M}_w/\bar{M}_n \simeq 1.1 \tag{11}$$

Thus

$$[\mathrm{HI}]_D - 1 \ll [\mathrm{HI}]_M - 1 \tag{12}$$

Consequently the block polymer molecules in the domain space tend to be packed so as to compensate the molecular weight distribution. This effect is most spectacular in the high regularity of the microdomains for binary mixtures of two block polymers with different molecular weights.[6,7,21,22]

For example, Figure 3 shows a typical electron micrograph of the solvent-cast films of a binary mixture of SIL-1 and SIL-2, containing 75 wt % SIL-1. SIL-2 is living anionically polymerized PS–PI diblock polymer with $\bar{M}_n = 1.8 \times 10^5$ and $W_{PS} = 0.53$. The mixture of the two block polymers with different molecular weights exhibits only a single morphology, such as shown in Figure 3, throughout the sample space, i.e., very regularly arranged alternating lamellae composed of PS and PI with a single identity period $\bar{D}$.

Figure 3 is a proof of the absence of demixing between SIL-1 and SIL-2. It also proves the existence of well-developed long-range order even in the mixture. The order existing in the mixture is identical with that found in pure block polymers. The single-crystalline regions of the lamellae are larger than 10 μm and sometimes even larger than the low-magnification limit of the electron microscope with which the individual lamellae can be resolved.

In the SAXS profiles from this mixture a total of 10 scattering maxima, which are all reduced to a single identity period, were observed.[22] The spacing $\bar{D}$ of the superlattice for the mixture (520 Å) lies between those for SIL-1 and SIL-2 (460 and 780 Å, respectively) and satisfies eq 2b. The observation strongly suggests that the two block polymers are molecularly mixed to form the single lamellar morphology, with its spacing being characterized by the number-average molecular weight $\bar{M}_n$ of the mixture. The results found for the solvent-cast films are in accordance with those found by Hadziioannou and Skoulios[6] for films prepared by freeze-drying dilute solutions of the mixtures with subsequent molding of the solid residues under shear stress. The detailed analysis of the SAXS profiles of the mixtures, which clearly show the 10th-order maxima, has been presented elsewhere.[22]

A question will naturally be raised concerning the molecular weight difference of the two polymers within which

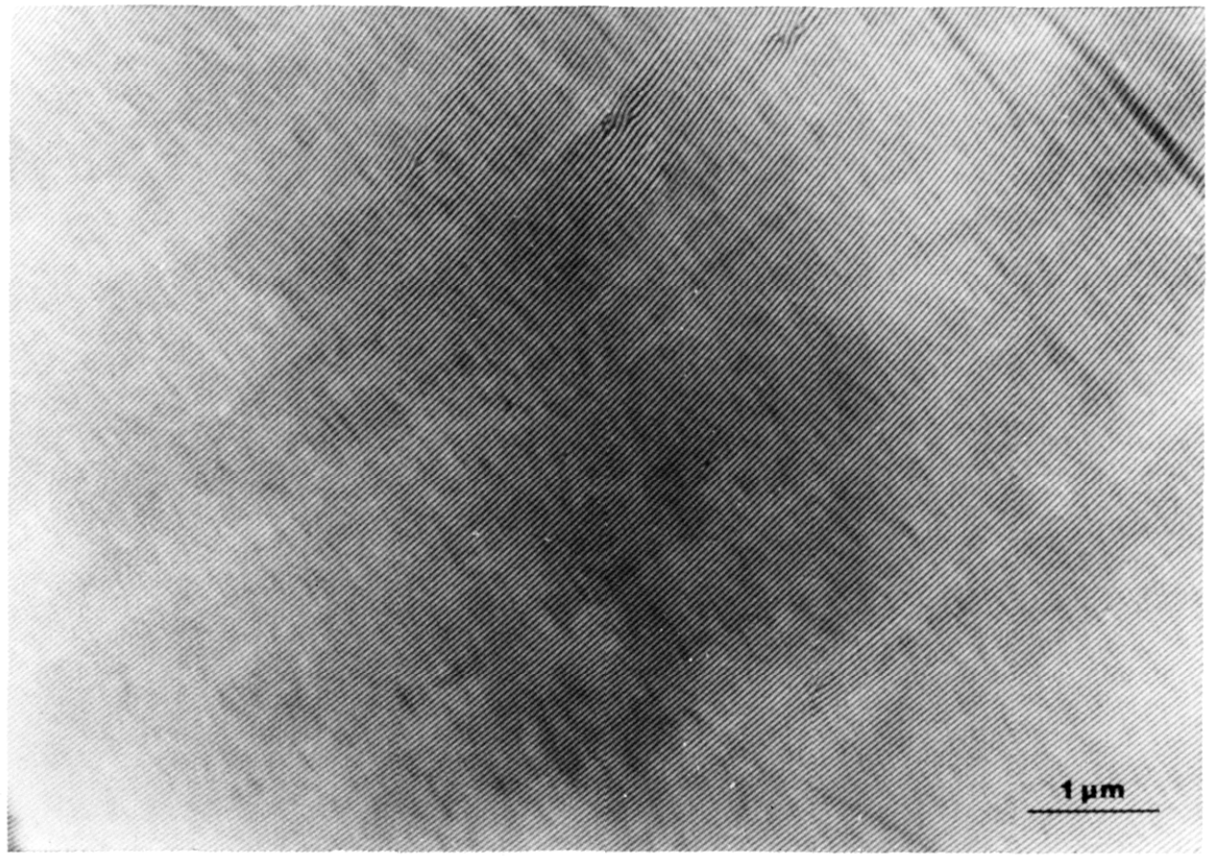

Figure 3. Transmission electron micrograph of an ultrathin section of the solvent-cast film of a mixture of SIL-1 and SIL-2 (75/25 by wt %) (OsO_4 stained).

they dissolve molecularly to form a single domain morphology. The answers to this problem will be discussed elsewhere.[21]

Equations 9 and 10 are applicable also to other morphologies such as cylindrical and spherical microdomains, where D can be taken as the interdomain distance. For cylindrical and spherical systems, the g value is generally a tensor quantity[16] $\{g_{ik}\}$ (i, k = 1, 2, 3), but if the paracrystalline distortion is assumed to be isotropic, the distortion can be represented by a single parameter g, as in eq 9 and 10.

Generally cylindrical and spherical microdomain systems seem to have long-range order less than that of the lamellar microdomain systems, giving rise to a smaller number of scattering maxima arising from the superlattice. The heterogeneity index $[HI]_D$ seems to increase with the dimensionality of the superlattice for the same $[HI]_M$.

Spherical domain systems form either a simple-cubic (sc) or a body-centered-cubic (bcc) superlattice whose relative peak positions of the scattering maxima are given by $1:2^{1/2}:3^{1/2}:4^{1/2}:5^{1/2}:6^{1/2}:\ldots$. A number of scattering maxima and shoulders were experimentally observed at the predicted angular positions,[4,9,23-25] normally[4,9,23] up to $4^{1/2}$ and in extreme cases up to $5^{1/2}$ for the simple-cubic lattice[24] and $6^{1/2}$ for the body-centered-cubic lattice.[25] The relation between the order of the distinguishable scattering maximum and the g value is not identical with the relation in eq 4 for the one-dimensional paracrystalline lattice. The relation has to be determined quantitatively on the basis of the cubic lattice systems with paracrystalline distortion of the second kind. Preliminary results obtained by computer simulations under the assumption of the isotropic distortion g indicated that the condition for the $\langle hkl \rangle$ diffraction being distinguishable is roughly given by[26]

$$g(h^2 + k^2 + l^2)^{1/2} \lesssim 0.24 \quad (13)$$

for sc and bcc. It should be noted that for bcc the extinction rule demands the appearance of the diffraction maxima in the order of (110), (200), (211), (220), (301), etc. with increasing the scattering angle. Consequently if the peak at $4^{1/2}$ is distinguishable in sc, it is expected that $g \lesssim 0.12$. In the case of bcc, the peak at $4^{1/2}$ relative to the first-order peak corresponds to (220) and hence $g \lesssim 0.085$; the corresponding heterogeneity indices $[HI]_D$ calculated from eq 9 are 1.014 and 1.007 respectively for sc and bcc, clearly satisfying eq 12 in any case. Similar arguments can be applied to the cylindrical systems. If the domains are in the hexagonally close-packed superlattice, the maxima from the superlattice should appear at $1:3^{1/2}:7^{1/2}:9^{1/2}:\ldots$ relative to the first-order maximum. A number of scattering maxima and shoulders were experimentally found at the predicted angular positions,[5,25,27-29] normally[5,27,28] up to $7^{1/2}$ and in the extreme case[25,29] up to $9^{1/2}$. The relation between g and n, as given by eq 4 and 13, has not been explored yet, but it is expected that the cylindrical systems will also satisfy eq 12.

Acknowledgment. We are grateful to Dr. M. Shibayama for assistance in this work. This work is partially supported by a scientific grant from the Japan Securities Scholarship Foundation.

Registry No. (Styrene)·(isoprene) (copolymer), 25038-32-8.

References and Notes

(1) Sadron, C.; Gallot, B. *Makromol. Chem.* **1973**, *164*, 301.
(2) Hoffmann, M.; Kämpf, G.; Krämer, H.; Pampus, G. *Adv. Chem. Ser.* **1971**, *No. 99*, 351.
(3) Hashimoto, T.; Shibayama, M.; Kawai, H. *Macromolecules* **1980**, *13*, 1273.
(4) Hashimoto, T.; Fujimura, M.; Kawai, H. *Macromolecules* **1980**, *13*, 1660.
(5) Mori, K.; Hasegawa, H.; Hashimoto, T., to be submitted to *Macromolecules*.
(6) Hadziioannou, G.; Skoulios, A. *Macromolecules* **1982**, *15*, 267.

(7) Hashimoto, T. *Macromolecules* **1982**, *15*, 1548.
(8) Richards, R. W.; Thomason, J. L. *Macromolecules* **1983**, *16*, 982.
(9) Bates, F. S.; Berney, C. V.; Cohen, R. E. *Macromolecules* **1983**, *16*, 1101.
(10) Meier, D. J. *J. Polym. Sci., Part C* **1969**, *26*, 81.
(11) Helfand, E. *Macromolecules* **1975**, *8*, 552.
(12) Hashimoto, T.; Shibayama, M.; Kawai, H. *Macromolecules* **1983**, *16*, 1093.
(13) Shibayama, M.; Hashimoto, T.; Kawai, H. *Macromolecules*, **1983**, *16*, 1434.
(14) Hashimoto, T.; Suehiro, S.; Shibayama, M.; Saijo, K.; Kawai, H. *Polym. J.* **1981**, *13*, 501.
(15) Fujimura, M.; Hashimoto, T.; Kawai, H. *Mem. Fac. Eng., Kyoto Univ.* **1981**, *43* (2), 166.
(16) Hosemann, R.; Bagchi, S. N. "Direct Analysis of Diffraction by Matter"; North-Holland Publishing Co.: Amsterdam, 1962.
(17) Such examples of the SAXS profiles for different block polymers are shown in Figure 4 in ref 18 and Figure 7 in ref 19. The highest order maximum reported for lamellae so far is the 15th for PS–PI block polymer having a total molecular weight of 3×10^5.[20]
(18) Hashimoto, T.; Todo, A.; Itoi, H.; Kawai, H. *Macromolecules* **1977**, *10*, 377.
(19) Hashimoto, T.; Nakamura, N.; Shibayama, M.; Izumi, A.; Kawai, H. *J. Macromol. Sci. Phys.* **1980**, *B17*, 389.
(20) Skoulios, A. E. In "Block and Graft Copolymers"; Burke, J. J., Weiss, V., Eds.; Syracuse University Press: Syracuse, NY, 1963.
(21) Hasegawa, H.; Yamasaki, K.; Hashimoto, T., to be submitted to *Macromolecules*.
(22) Hasegawa, H.; Hashimoto, T. *Kobunshi-Ronbunshyu* **1984**, *41*, 759.
(23) Bates, F. S.; Cohen, R. E.; Berney, C. V. *Macromolecules* **1982**, *15*, 589.
(24) Shibayama, M.; Hashimoto, T.; Kawai, H. *Macromolecules* **1983**, *16*, 16.
(25) Tanaka, H.; Hasegawa, H.; Hashimoto, T., to be submitted to *Macromolecules*.
(26) Unpublished results.
(27) Keller, A.; Pedemonte, E.; Willmouth, F. M. *Nature (London)* **1970**, *225*, 538; *Kolloid Z. Z. Polym.* **1970**, *238*, 385.
(28) Lewis, P. R.; Price, C. *Polymer* **1971**, *12*, 258.
(29) Richards, R. W.; Thomason, J. L. *Polymer* **1981**, *22*, 581.

Dynamics of Wormlike Chains

Sergio R. Aragón S† and R. Pecora*

Department of Chemistry, Stanford University, Stanford, California 94305.
Received January 8, 1985

ABSTRACT: The dynamics of free-draining polymers in dilute solution are treated with the Kratky–Porod wormlike chain model. The model consists of differentiable space curves of constant length with bending elasticity. We show that eliminating the stretching elasticity gives an internally consistent model which satisfies the pure bending Langevin equation of motion. The dynamical equation is solved by a normal mode analysis representing the transverse vibrations of an elastic curve with free ends. A time-independent Green's function is used to calculate the pair correlation function, giving all equilibrium properties of the model. The same techniques are applied to the time-dependent case. All properties depend on one parameter, the persistence length, λ^{-1}, of the polymer. As an example, the polarized light scattering from a dilute solution of isotropic random coils is calculated in detail. The model requires the separate treatment of the rotational and the internal flexing degrees of freedom of the polymer. Its main area of application will be in the description of the dynamics of dilute solutions of semiflexible macromolecules.

I. Introduction

The concept of a random flight chain is a key concept in understanding polymer solution properties for very flexible polymers. The model most widely used to describe the dynamics of such flexible chains is the famous "spring and bead" model proposed originally by Rouse[1] and Bueche.[2] The dynamical consequences of this model were developed mainly by Zimm,[3] who applied it to the viscoelasticity, flow birefringence, and dielectric relaxation in dilute polymer solutions. Other properties such as the dynamic light scattering of the optically isotropic Rouse model were given by Pecora[4] and Saito,[5] and for optically anisotropic Rouse polymers (in the forward scattering limit) by Ono and Okano.[6] The success of the Rouse–Zimm model in most of these areas is well-known and a good account is given in Yamakawa's[7] thorough exposition of dilute polymer solution theory.

Nevertheless, the Rouse model, apart from the considerations of excluded volume and hydrodynamic interaction effects, does have limitations. Obviously it is only applicable to very flexible molecules, yet there is great interest in both natural and synthetic polymers with intermediate degrees of flexibility between the random coil and the rigid rod. In addition, as Harris and Hearst[8] have pointed out, the Rouse model, even for very flexible molecules, is inappropriate for high-frequency phenomena since in this case any real molecule looks increasingly rigid and the assumption of Gaussian statistics for the bead separations breaks down. Finally, a related problem is that the number of beads used to model a polymer molecule is arbitrary; thus, only the slow relaxations of a polymer molecule can be treated since the results of any calculations must be independent of the actual number of beads chosen.

With these considerations in mind, Harris and Hearst[8] introduced the Kratky–Porod[9] wormlike chain, treated as a differentiable space curve with bending elasticity, to account for the presence of stiffness in a linear polymer molecule. The wormlike chain model contains one main parameter, the persistence length, λ^{-1}, which is simply related to the bending elasticity constant,[10] ϵ, by $\lambda = kT/2\epsilon$.

Given a polymer of contour length L, the rigid-rod limit corresponds to $\lambda L \to 0$, whereas the random-coil limit corresponds to $\lambda L \to \infty$. This model, in addition to covering the whole range of flexibilities, resolves the difficulties of the Rouse model in the high-frequency region because the statistics are not Gaussian. Nevertheless, in our version of this model, we neglect hydrodynamic and

†Permanent address: Department of Chemistry, Universidad del Valle, Guatemala, Guatemala.

0024-9297/85/2218-1868$01.50/0